Temperature and metal composition dependence of lateral photovoltaic effect in Al-Alq_3/SiO_2/Si structures

Chao Wang (王 超)[1,2], Junqiang Shao (邵军强)[1,2], Zelin Mu (穆泽林)[1,2], Wenming Liu (刘文明)[1,2], and Gang Ni (倪 刚)[1,2*]

[1]*Department of Optical Science and Engineering, Fudan University, Shanghai 200433, China*

[2]*Key Laboratory of Micro and Nano Photonic Structures (Ministry of Education), Fudan University, Shanghai 200433, China*

[*]*Corresponding author: gni@fudan.edu.cn*

Received January 7, 2014; accepted March 5, 2014; posted online April 4, 2014

A series of Al_x-$(Alq_3)_{1-x}$ granular films is prepared on Si wafer with native oxide layer using co-evaporation technique. Large lateral photovoltaic effect (LPE) is observed, with an optimal LPV sensitivity of 75 mV/mm in $x = 0.35$ sample. The dependence of LPE on temperature and Al composition is investigated, and the possible mechanism is discussed.

OCIS codes: 040.5160, 040.5350, 160.4890.
doi: 10.3788/COL201412.040402.

Metal-semiconductor (MS) and metal-oxide-semiconductor (MOS) devices have been widely used in the modern integrated circuit and solar cell industry. When sufficient energetic irradiation is incident on a p-n or MS/MOS junction, transverse photovoltaic effect can be observed, which is widely used in solar cells. Furthermore, if a nonuniform irradiation is applied on the junction, an additional photovoltage parallel to the plane of the junction can be obtained, which is called lateral photovoltaic effect (LPE)[1–5]. LPE has a wide range of applications, especially in position-sensitive detectors (PSDs).

In early studies, due to the high conductivity of metal layer, obvious metal layers LPE can only be observed in MOS/MS structures with nanoscale metal layers (about several nanometers), such as Ti/Si, Co/SiO_2/Si and Co/Si[6–8]. However, the nano-metal layer prone to oxidation in the air, which could affect the performance and working life of the devices. Recently, large LPE was also found in composite films on Si substrates[9–13]. As we know, the transport property of the composite films can be greatly influenced by the metal composition and temperature. However, the dependence of LPE on metal composition and temperature in composite films on Si wafer has not been reported yet. In this paper, we investigated the influence of temperature and metal composition on LPE in Al-Alq_3/SiO_2/Si structure, and discussed possible mechanisms.

The Al-Alq_3 layer was deposited on n-type Si(111) substrate using co-evaporation technique. Si substrates were covered with a thin native SiO_2 layer, and the resistivity of wafers was about 2–4 Ω·cm. Before deposition, the substrates were rinsed with distilled deionized water and cleansed with ethanol. The base pressure of the evaporation chamber was about 1×10^{-4} Pa. The evaporation rates of Al and Alq_3 were accurately controlled to obtain Al-Alq_3 granular films with different Al fractions. The thicknesses of the Al-Alq_3 layers were about 75 nm. Both the evaporation rate and the film thickness were determined by a quartz crystal thickness monitor (Sigma SQM-160).

The measurements were performed in an optical cryostat (Cryo industries) at different temperatures. The samples were cut into about 4×9 (mm) rectangles. Two indium electrodes were placed on the Al-Alq_3 film surface or the Si substrate. The samples were scanned spatially with a semiconductor laser (10 mW, 532 nm) focusing on a roughly 200-μm diameter spot at the surface in the dark. The schematic drawing of the experimental setup is shown in the bottom inset of Fig. 1. The lateral photovoltage (LPV) and resistivity were measured with a Keithley 2001 multimeter and a Keithley 238 sourcemeter, respectively. The microstructures of granular film samples were investigated by transmission electron microscopy (TEM, Jeol JEM-2010).

The TEM image of the as-deposited $Al_{0.35}(Alq_3)_{0.65}$ granular film sample is shown in the upper inset of Fig. 1. It exhibits the typical microstructural characteristic of granular films, where the randomly oriented granular Al particles are isolated by the Alq_3 molecules. The particle size is approximately 3–10 nm.

Figure 1 shows the dependence of the induced LPV on the position of light for $Al_{0.35}(Alq_3)_{0.65}$/SiO_2/Si sample, where V_{AB} represents the induced electric potential difference between the two indium electrodes on the film surface, and V_{CD} represents the potential difference on the Si substrate. A large LPV can be observed on the $Al_{0.35}(Alq_3)_{0.65}$ side in the sample, and the optimal LPV reaches about 180 mV near the electrodes. The open-circuit position sensitivity, i.e. the variation of the output voltage for 1 mm displacement of the laser spot[4], is about 75 mV/mm, which is close to the LPV values in inorganic LPE devices[7–11]. However, only small LPV can be observed on the Si side in the sample. In MS/MOS junctions, the resistivity and the Fermi level are considered to be the two crucial factors for the metal side LPE[8]. In our samples, due to the doping of Alq_3, Al particles are isolated by organic semiconductor Alq_3. The conductivity of the upper layer decreases greatly, leading to obvious LPE. For the sake of comparison, we

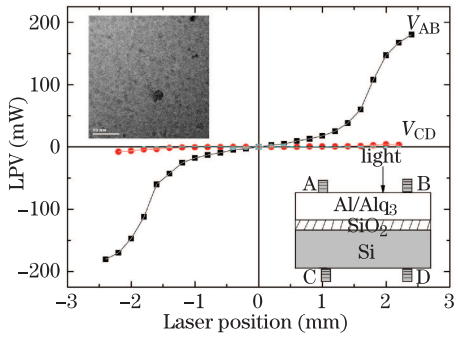

Fig. 1. Dependence of the induced lateral photovoltage on the position of light for $Al_{0.35}(Alq_3)_{0.65}/SiO_2/Si$ sample. The upper inset shows the TEM image of the sample and the bottom inset presents the schematic picture of the experimental setup.

also prepared a series of $Al/SiO_2/Si$ samples with different thicknesses of Al layers. The metal side LPEs are negligibly small in the $Al/SiO_2/Si$ samples with the thickness of Al layer being greater than 10 nm.

As shown in Fig. 1, V_{AB} and V_{CD} curves follow the same pattern, i.e. a monotonic increase with the laser position, which is different from the conventional LPE theory in p-n junctions, where LPV should be reversible on the two sides. The unusual irreversible LPE was also observed in $Bi_2Sr_2Co_2O_y/LaAlO_3$, LSMO/SNTO, Cu_2O/Si and Co-$Alq_3/SiO_2/Si$ structures[13−16]. When a beam of light hits the surface of Al-Alq_3 film, the electron-hole pairs are generated inside the Si substrate. Subsequently, the excited holes are swept into the upper granular film by the built-in field with electrons remaining in the Si substrate. Due to the nonuniform irradiation, the excited carrier concentration is much greater in the illuminated zone. Thus the excess holes on the Al-Alq_3 side will form a gradient of concentration between the illuminated and the nonilluminated zones, and a high electric potential will be measured near the laser spot, which is similar to the conventional LPE theory in p-n junction[4,9,17]. Meanwhile, the Dember effect dominates the LPE in the Si substrates. As a result of the partial block effect of the oxide layer, a part of separated holes still remain in the Si substrate. Because the mobility of electrons is greater than that of holes in silicon, the lateral distribution of separated electrons and holes are quite different in the Si substrate. The electrons are far away from the laser spot while the holes stay close to the light, which brings about a higher potential in the center of the laser spot, showing irreversible LPE. To finish a circulation, these light-induced holes in the upper layer will transit back to the semiconductor layer and recombine with the electrons in Si substrates at nonillumination positions. If the illumination remains, the stable photovoltage distributions can be formed in the upper layer and Si substrates[14]. Therefore, both of the Dember effect and the conventional LPE affect the distribution of the carriers in the system, giving rise to the above unusual LPE phenomenon.

The temperature dependence of LPE for the $Al_{0.35}(Alq_3)_{0.65}/SiO_2/Si$ sample is shown in Fig. 2(a). The LPV was measured on the fixed position of $x = 1.8$ mm with the temperature sweeping from 300 K to 50 K. With the decrease of temperature, the LPV increases from 300 to 110 K first, then keeps stable and decreases finally. The optimal LPV reaches 187 mV at 62 K.

In order to understand the above temperature dependence of LPE, the temperature dependence of the resistivity for the sample has been investigated, as shown in Fig. 2(b). With the decrease of temperature, the resistivity of the sample increases nonlinearly, showing a negative temperature coefficient of resistance (TCR). As seen in the inset of Fig. 2(b), where temperature axis is on a logarithmic scale, a logarithm of R plot is found well linearly proportional to T.

Recently, Wang *et al.*, proposed a theoretical model based on the conventional LPE theory for LPE of metal side in MS/MOS structures. The following is the equation describing the relationship between LPV and resistivity[18],

$$LPV(x) = 2KNC\sqrt{\rho}\cdot\exp(-LC\sqrt{\rho})x, \quad (-L < x < L), \tag{1}$$

where K is the proportional coefficient, x is the laser position, $-L$ and L are the positions of the two contacts, C is a related coefficient, and ρ presents the resistivity.

As discussed above, the conventional LPE mechanism is dominat in LPE in the upper layer. Thus, Eq. (1) can be used to fit our experimental results in Fig. 2. Figure 3 shows the LPV as a function of resistivity, where the red solid curve is the fitting result. The equation is found to fit the experimental data well, indicating the proper mechanism selected for the upper side LPE of samples. With the decrease of temperature, the resistivity of Al-Alq_3 layer increases significantly. Consequently, the separated holes diffuse slowly, resulting in a high potential distribution in the plane of film, showing larger LPV. However, with the further decrease of temperature, few of holes are able to diffuse to the nearby electrode because of the very high resistivity at low temperatures. Thus the densities of holes at the two contacts are both

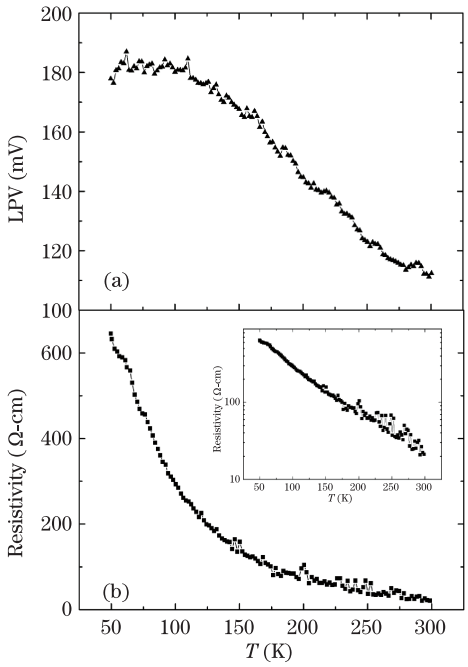

Fig. 2. (a) Temperature dependence of LPV; (b) temperature dependence of resistivity for $Al_{0.35}(Alq_3)_{0.65}/SiO_2/Si$ sample.

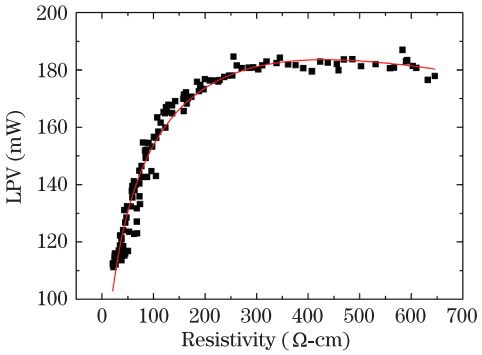

Fig. 3. LPV as a function of resistivity of $Al_{0.35}(Alq_3)_{0.65}/SiO_2/Si$ samples. The red smooth curve shows the result of fitting.

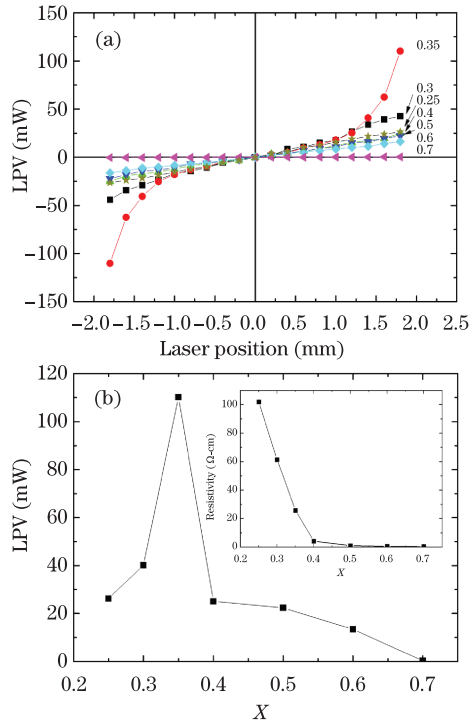

Fig. 4. (a) LPV curves for $Al_x(Alq_3)_{1-x}/SiO_2/Si$ samples with different volume fractions of Al; (b) resistivity as a function of the volume fraction of Al in $Al_x(Alq_3)_{1-x}/SiO_2/Si$ samples.

low, also resulting in a small LPV[9].

As is known to us, the metal composition plays important roles in granular films, and could strongly influence the microstructures and transport properties. Since the LPE is closely related to the conductance of the upper layer in MS/MOS structures, it is interesting to investigate the dependence of LPE on Al composition in the samples. The position dependence of LPV for a series of samples with different Al compositions at room temperature is shown in Fig. 4(a), where LPV denotes the LPV between the indium electrodes on the granular films. Similar to the above sample ($x = 0.35$) obvious LPE can be observed in most samples. The LPEs are strongly influenced by the change of Al fractions. For the sample with a high Al composition, LPV is very small, only about 0.3 mV at $x = 0.7$. With the decrease of Al fraction, LPV increases rapidly, reaching an optimal value of 112 mV (for $x = 0.35$ sample, at 1.8 mm). However, with the further decrease of Al fraction, the LPV decreases accordingly. We plotted the curve of the dependence of LPE on Al composition, as shown in Fig. 4(b). The inset of Fig. 4(b) shows the resistivity as a function of Al volume fraction. With the increase of Al fraction, the resistivity of the samples drops rapidly. When $x > 0.4$, the resistivity goes down slowly with the further increase of x. This indicates that the percolation threshold of the system is around 0.4. In samples with high x, the neighboring Al granules interconnect and form a continuous conductive network, showing metal conductive behaviors. When the light impinges the surface of the sample, the separated holes can easily diffuse from the illuminated zone to the nonilluminated zone in the upper layer, resulting in a small difference of electric potential between the two contacts, i.e., a small LPV[9]. With the decrease of Al fraction, more and more Al granules begin to be isolated by Alq_3 matrix. The sample gradually shows low conductive behaviors on account of the low conductivity of Alq_3, resulting in a larger LPV. Especially in the $x = 0.35$ sample, which is slightly below the percolation threshold, the largest LPV is obtained. With the further decrease of x, the diluted metal granules are entirely surrounded by Alq_3 matrix, showing an insulating conductive behavior. Then the carriers can hardly diffuse due to the large resistivity, leading to a reduced LPV. Furthermore, the weakening of the built-in field may also contribute to the decrease of LPV in samples with lower x. In consequence, instead of varying the thickness of metal layers in previous MS/MOS junctions, we can adjust the metal composition of the granular films to obtain an optimal LPE in our structures, which may be beneficial in the application of PSDs.

In conclusion, we fabricated a series of Al_x-$(Alq_3)_{1-x}$ granular films on Si wafer, and observed large lateral photovoltaic effect in the structure. We also investigated the dependence of LPE on temperature and metal composition, and discussed the possible mechanisms.

This work was supported by the National Natural Science Foundation of China under Grant No. 61076093.

References

1. W. Schottky, Phys. Z. **31,** 913 (1930).
2. J. T. Wallmark, Proc. IRE **45,** 474 (1957).
3. J. Henry and J. Livingstone, J. Mater. Sci.-Mater. Electron. **12,** 387 (2001).
4. K. Zhao, K. J. Jin, H. B. Lu, Y. L. Huang, Q. L. Zhou, M. He, Z. H. Chen, Y. L. Zhou, and G. Z. Yang, Appl. Phys. Lett. **88,** 141914 (2006).
5. Z. Q. Lu, K. Zhao, H. Liu, N. Zhou, H. Zhao, L. Gao, S. Q. Zhao, and A. J. Wang, Chin. Opt. Lett. **7,** 718 (2009).
6. R. H. Willens, Appl. Phys. Lett. **49**, 663 (1986).
7. S. Q. Xiao, H. Wang, Z. C. Zhao, Y. Z. Gu, Y. X. Xia, and Z. H. Wang, Opt. Express **16,** 3798 (2008).
8. C. Q. Yu, H. Wang, S. Q. Xiao, and Y. X. Xia, Opt. Express **17**, 21712 (2009).
9. C. Q. Yu and H. Wang, Sensor **10,** 10155 (2010).
10. H. Wang, S. Q. Xiao, C. Q. Yu, Y. X. Xia, Q. Y. Jin,

and Z. H. Wang, N. J. Phys. **10**, 093006 (2008).
11. J. Lu and H. Wang, Opt. Express **19,** 13806 (2011).
12. W. W. Liu, S. Q. Zhao, K. Zhao, and W. Sun, Int. J. Photoenergy **2010,** 793481 (2010).
13. W. M. Liu, Y. Zhang, and G. Ni, Opt. Express **20,** 6225 (2012).
14. K. J. Jin, H. B. Zhao, H. B. Lu, L. Liao, and G. Z. Yang, Appl. Phys. Lett. **91**, 081906 (2007).
15. L. Du and H. Wang, Opt. Express **18,** 9113 (2010).
16. G. Y. Yan, G. S. Fu, Z. L. Bai, and S. F. Wang, Chin. Opt. Lett. **11,** 123101 (2013).
17. J. Du, H. Ni, K. Zhao, Y. C. Kong, H. K. Wong, S. Q. Zhao, and S. H. Chen, Opt. Express **19,** 17260 (2011).
18. C. Q. Yu, H. Wang, and Y. X. Xia, Appl. Phys. Lett. **95,** 263506 (2009).